Photon strength functions of ^{156}Gd from radiative capture of resonance neutrons

B. Baramsai,[1,2,*] J. Kroll,[3] G. E. Mitchell,[1,2] U. Agvaanluvsan,[4] F. Bečvář,[3] T. A. Bredeweg,[5] A. Chyzh,[1,2] A. Couture,[5] D. Dashdorj,[4] R. C. Haight,[5] M. Jandel,[5] A. L. Keksis,[5] M. Krtička,[3] J. M. O'Donnell,[5] R. S. Rundberg,[5] J. L. Ullmann,[5] D. J. Vieira,[5] and C. L. Walker[1,2]

[1]*North Carolina State University, Raleigh, North Carolina 27695, USA*
[2]*Triangle Universities Nuclear Laboratory, Durham, North Carolina 27708, USA*
[3]*Charles University in Prague, CZ-180 00 Prague 8, Czech Republic*
[4]*MonAme Scientific Research Center, P.O.Box 24-603, Ulaanbaatar, Mongolia*
[5]*Los Alamos National Laboratory, P.O. Box 1663, Los Alamos, New Mexico 87545, USA*

(Received 11 July 2012; published 15 April 2013)

The ^{155}Gd(n,γ) reaction was measured with the DANCE γ-ray calorimeter (consisting of 160 BaF_2 scintillation detectors) at the Los Alamos Neutron Science Center. The γ-ray energy spectra for different multiplicities were obtained for the s-wave resonances. The shapes of these spectra were compared with simulations based on the use of the DICEBOX statistical model code. Simulations showed that the photon strength functions (PSFs) successfully describing the decay of ^{156}Gd are very similar to the PSFs describing the decay of previously published ^{158}Gd results. It was demonstrated that the scissors mode is required not only for the ground-state transitions, but also for transitions between excited states.

DOI: 10.1103/PhysRevC.87.044609 PACS number(s): 28.20.Np, 27.60.+j, 25.40.Lw, 25.40.Ny

I. INTRODUCTION

In medium and heavy mass nuclei detailed information about the properties of nuclear levels and transitions between them usually exists only at low excitation energies near the ground state. In this region, the spacing between levels is sufficient to clearly observe these levels. As the level density increases with excitation energy, it becomes difficult to resolve transitions to or from the individual levels. Obtaining reliable spectroscopic information on these levels, which form the so-called quasicontinuum, becomes very difficult.

It is believed that properties of the nucleus in the quasicontinuum can be described by the extreme statistical model in terms of the nuclear level density (NLD) and a set of photon strength functions (PSFs) for different multipolarities. These quantities are important for the correct description of reaction rates in many different reactions and are especially needed in nuclear astrophysics and in the development of advanced nuclear reactors.

One of the ways to examine the PSFs and NLD in the quasicontinuum region is via study of the properties of spectra of γ rays accompanying neutron capture at isolated neutron resonances. The present paper is focused on obtaining information on the PSFs and NLD of ^{156}Gd. The γ-ray spectra were measured at isolated s-wave neutron resonances in the ^{155}Gd$(n,\gamma)^{156}$Gd reaction using DANCE, the Detector for Advanced Neutron Capture Experiments [1,2]. This highly segmented, highly efficient γ calorimeter is installed at the pulsed neutron beam at LANSCE (the Los Alamos Neutron Science Center) at Los Alamos National Laboratory. The neutron time-of-flight technique was used to resolve the neutron resonances.

This experiment is a part of a series of experiments that measure neutron capture on all of the stable gadolinium isotopes. The primary aim of this study is to obtain more systematic information about the scissors mode: a resonance in the magnetic dipole PSF at $E_\gamma \sim 3$ MeV. In addition, we want to determine the energy dependence of the electric dipole PSF. Results for the PSFs and NLD in the neighboring even-even isotope ^{158}Gd obtained with the same experimental setup have recently been published [3].

In Sec. II the experimental technique to measure the γ spectra with the DANCE calorimeter is described. The modeling of the statistical γ cascades is discussed in Sec. III. Information about the PSFs and NLD that can be obtained from the measured γ-ray spectra is presented in Sec. IV and briefly compared with other available data in Sec. V. A summary is provided in Sec. VI.

II. EXPERIMENT

A detailed description of the experimental setup and data processing is given in [4]; here we describe only the basic features related to the experimental spectra studied in this paper.

A. Experimental setup

The experiment was performed at the neutron source LANSCE [5]. The pulsed 800 MeV H^- beam from the LANSCE linear accelerator was injected into the proton storage ring after being stripped to H^+ by a thin foil. The average current was 100 μA. This pulsed beam was then extracted with a repetition rate of 20 Hz and struck a tungsten spallation target. The resulting fast neutrons were moderated in the upper-tier water moderator and sent to flight path 14 at the Manuel Lujan Jr. Neutron Scattering Center. The DANCE detector array is installed at 20 m on this flight path.

The DANCE spectrometer [1,2] is designed for studying neutron capture cross sections on small samples. DANCE

*bbarams@ncsu.edu

consists of 160 BaF_2 scintillation crystals surrounding a sample and covering a solid angle of $\simeq 4\pi$. Each crystal serves as a γ spectrometer. A ^{6}LiH shell 6-cm thick is placed between the sample and the BaF_2 crystals in order to reduce the scattered neutron flux striking the crystals. The remaining background due to scattered neutrons that penetrate the ^{6}LiH shell and interact with the BaF_2 crystals is subtracted in the offline analysis. This background is very small in the data used in the present analysis. In addition to the BaF_2 crystals, the DANCE setup includes two additional detectors that are used to monitor the neutron flux—a proportional counter filled with BF_3+Ar gas, and an n-type surface barrier Si detector which views a thin ^{6}LiF deposit—and a ^{235}U fission chamber.

As described in Ref. [4], the ^{155}Gd target was prepared at the Oak Ridge National Laboratory as a self-supporting metal foil with an area $S = 5.064$ cm^2 and areal density $n = 1.008$ mg/cm^2. The ^{155}Gd target (natural abundance 14.80%) was enriched to 91.74%; the major contaminants were ^{154}Gd (0.63%), ^{156}Gd(5.12%), ^{157}Gd (1.14%), and ^{158}Gd (0.94%). Data were accumulated for about 130 hours.

B. Data processing

The DANCE acquisition system [6] is based on digitization of signals from all 160 detectors using four-channel Acqiris DC265 digitizers with a sampling rate of 500 mega samples per second.

Intensities of the fast (decay time $\approx$600 ps) and slow (decay time $\approx$600 ns) components of the scintillation signal from a specific BaF_2 crystal are collected independently. The ratio of these two components of the signal can be used for discrimination against the α background from natural radioactivity of Ra in the BaF_2 crystals [2].

The energy calibration of the DANCE crystals was performed with a combination of γ-ray sources: ^{137}Cs, ^{88}Y, ^{22}Na, and the intrinsic radioactivity in the BaF_2 crystals due to ^{226}Ra and its daughters. The latter calibration was conducted on a run-by-run basis to provide the energy alignment of all crystals in the offline analysis.

Typical spectra of sums of deposited γ-ray energies, hereafter called *sum-energy spectra*, are shown in Fig. 1. As only s-wave neutron capture plays a role at low neutron energies in this mass region, in this experiment we observe only resonances with $J^\pi = 1^-$ and 2^-. There is a small difference between the contributions of different multiplicities M of emitted γ radiation for resonances with different spins; this was exploited to determine spins of ^{155}Gd resonances in Ref. [4].

Each sum-energy spectrum consists of (i) a peak near the full available energy from the neutron capture reaction, which is close to the neutron separation energy $S_n = 8.536$ MeV, and (ii) a low energy tail that corresponds to γ cascades for which a part of the emitted energy escaped the detector array. The position of the peak is shifted down with respect to S_n due to the strong contribution of internal electron conversion for transitions between the lowest lying levels of ^{156}Gd. The shape of the spectrum at low sum energies (below about 3 MeV) is strongly influenced by the background from natural β activity in the BaF_2 crystals, especially for low multiplicities. As only

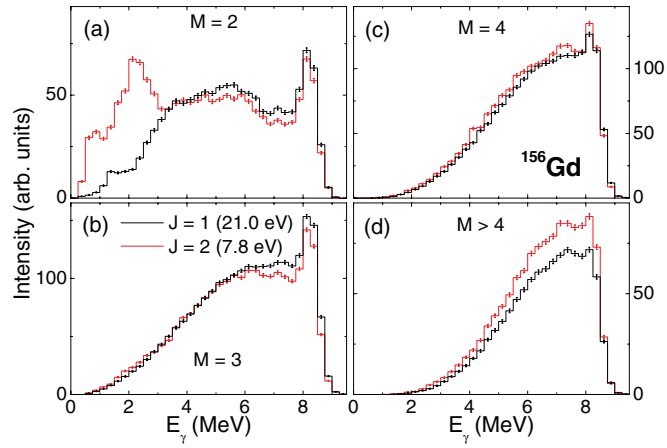

FIG. 1. (Color online) Examples of sum-energy spectra for resonances at neutron energies of 21.0 and 7.8 eV with J^π assignments 1^- and 2^-, respectively. The cluster multiplicities of the γ cascades, M, are indicated. All spectra are normalized as described in Sec. II B.

events with higher sum energy are used in the analysis, in practice this background is not important.

Often an emitted capture γ ray does not deposit its full energy in one crystal. Thus the number of crystals that fire is usually higher than the true multiplicity of a capture event. Therefore all contiguous crystals that have fired during an event are combined into *clusters* and considered as the response of the detector array to a single γ ray. The number of clusters observed in a capture event is called the "cluster multiplicity". This multiplicity is much closer to the true multiplicity of the γ cascade than is the "crystal multiplicity" (the total number of crystals that fire).

Only events corresponding to strong resonances were analyzed. These resonances were easily identified from the time-of-flight spectrum. In addition, only events contributing to the energy range of 7.6–8.6 MeV in the sum-energy spectra were considered in further analysis.

With these constraints we constructed what we call spectra of multistep γ cascades (MSCs) and spectra of *gated* MSCs.

For a given multiplicity M, the MSC spectrum is understood to be a spectrum of γ-ray energies deposited in M detector clusters. Gated MSC spectra are constructed in a similar way, but with the additional condition that the deposited energy in one of M detector clusters is in an *a priori* chosen *gating energy range*. In such a case the deposited energy in this cluster is ignored and only energies deposited in the other clusters contribute to a gated MSC spectrum of interest. If the deposited energy in more than one cluster falls into the chosen gating energy range, only the one which is closest to the midpoint of the range is ignored.

The use of a wider interval of detected energy sums improves the experimental statistics in the constructed spectra, but leads to significant smearing of interesting structures observed in the MSC spectra. On the other hand, narrowing the interval has no strong impact on the spectral shape and only reduces the statistical precision.

To facilitate the comparison of the data with model predictions, all sum-energy and MSC spectra for a given

resonance were normalized using one common factor. In this way it was ensured that the integral of the sum-energy spectrum for $M = 2$–7 in the γ-ray energy range 7.6–8.6 MeV had a common value for all resonances.

In general, there is a background contribution in the MSC and gated MSC spectra that primarily originates from γ rays following the capture of scattered neutrons in the various barium isotopes in the BaF_2 detectors. There is only a very small contribution from capture in other Gd isotopes in the target. The size of this background can be estimated using events corresponding to energies above about 9 MeV in the sum-energy spectrum in the same manner as described in Ref. [4]. For spectra from the strong resonances used in the present analysis of PSFs, this background contribution is negligible.

III. SIMULATION OF THE γ DECAY OF ^{156}Gd

MSC and gated MSC spectra carry important information on the PSFs and the NLD; they are the results of a complicated interplay of these quantities. Unfortunately, the PSFs and the NLD cannot be obtained directly from the spectra. We adopted a trial-and-error approach in which we compared experimental quantities with the outcome of simulations based on various models for the PSFs and the NLD. This comparison can tell us which of the PSFs and NLD models are most likely to be valid.

A. Simulations of spectra

The γ cascades following resonance neutron capture were generated using the DICEBOX algorithm [7] under various assumptions about the NLD and PSFs. The response of the DANCE detector to each generated cascade was subsequently obtained from a simulation made with the aid of the GEANT4 code [8]. The resulting simulated MSC and gated MSC spectra were then compared with their experimental counterparts.

In the DICEBOX algorithm, below some critical energy, $E_{\rm crit}$, all of the characteristics of the decay scheme, i.e., energies, spins and parities of levels, as well as their decay properties, are taken from existing experimental data. The choice of the critical energy was made with care to guarantee that all of the information for energies below $E_{\rm crit}$ is complete. We took the required data on low-lying levels from [9] and adopted $E_{\rm crit} = 1.95$ MeV. Above $E_{\rm crit}$ the level system of the nucleus and its complete decay scheme are generated using an *a priori* chosen NLD function $\rho(E, J, \pi)$ and PSFs for multipolarities $E1$, $M1$, and $E2$. All higher multipolarities are neglected. The partial radiation width $\Gamma_{a\gamma b}$ for a transition between an initial level a and a final level b is given by

$$\Gamma_{a\gamma b} = \sum_{\rm XL} \frac{\xi_{\rm XL}^2 f^{\rm (XL)}(E_\gamma, \Theta) E_\gamma^{2L+1}}{\rho(E_a, J_a, \pi_a)}, \qquad (1)$$

where $f^{\rm (XL)}$ stands for the photon strength functions for transitions of type X (electric or magnetic) and multipolarity L, and $\xi_{\rm XL}$ is a random number generated from a normal distribution with zero mean and unit variance. This random number ensures that the individual widths $\Gamma_{a\gamma b}$ fluctuate according to the Porter-Thomas distribution [10]. The argument Θ of the $f^{\rm (XL)}$ stands for additional quantities that the PSF may depend on other than E_γ: some of the models depend on the level's excitation energy (see Sec. III B). The sum in Eq. (1) is over all allowed types and multipolarities of transitions. Internal electron conversion, which is important in transitions between the lowest excited states in ^{156}Gd, is correctly treated in the DICEBOX algorithm [7].

Hereafter the simulated system of all levels and their decay scheme is called a *nuclear realization*. Due to the Porter-Thomas fluctuations there is an infinite number of nuclear realizations that differ from each other even for fixed PSFs and NLD models.

These different nuclear realizations can be simulated with the DICEBOX code. For each model typically 20 nuclear realizations, each with 100 000 cascades, were simulated for the initial spins of s-wave resonances, i.e., for levels with spins $J^\pi = 1^-$ and 2^- at an excitation energy equal to S_n. The results do not change if the number of realizations increases.

Among the various kinds of information that can be obtained from the combined DICEBOX+GEANT4 simulations, in the present work we are especially interested in the MSC and gated MSC spectra; see Sec. IV. In addition, the total radiation width, which is obtained directly from DICEBOX simulations, is used in the comparison described in Sec. V.

B. Photon strength functions

1. Electric-dipole transitions

Neutron resonance decay is dominated by dipole transitions. It is well known that for γ-ray energies above neutron separation energies the electric-dipole ($E1$) transitions play a major role. The PSF at these energies in axially deformed nuclei seems to be consistent with the sum of two Lorentzian terms,

$$f_{\rm SLO}^{(E1)}(E_\gamma) = \frac{1}{3(\pi\hbar c)^2} \sum_{i=1}^{2} \frac{\sigma_{G_i} E_\gamma \Gamma_{G_i}^2}{\left(E_\gamma^2 - E_{G_i}^2\right)^2 + E_\gamma^2 \Gamma_{G_i}^2}. \qquad (2)$$

Here E_{G_i}, Γ_{G_i}, and σ_{G_i} are the parameters of the giant electric dipole resonance (GEDR) which is split into two components ($i = 1$ and 2) in axially deformed nuclei. The parameters $E_G = 12.27$ and 15.94 MeV, $\Gamma_G = 2.95$ and 5.70 MeV, and $\sigma_G = 181$ and 215 mb were adopted; they come from a fit of data from the (γ,n) reaction on the ground state of the nearby nucleus ^{154}Sm [11] (data from this type of reaction are not available for ^{156}Gd.). Adopting parameters from a neighboring nucleus seems justified, as the GEDR parameters are believed to vary only slightly for nuclei with similar masses and deformations. For instance, the fit of ^{160}Gd (γ, n) data [11] at energies below about 9 MeV gives an $f^{(E1)}$ nearly indistinguishable from the fit to (γ, n) data on ^{154}Sm. The model given by Eq. (2) is known as the Brink-Axel or Standard Lorentzian (SLO) model.

Although there is essential agreement on the energy dependence of the giant resonance at higher energies, the shape of the $E1$ PSF below the neutron separation energy is not well known. There exist many available models and parametrizations of the $E1$ PSF in this region of γ-ray energies which modify the Lorentzian shape of the low-energy tail of

GEDR. Usually one of two models is used. The first one was proposed by Kadmenskij, Markushev and Furman [12] for description of the $E1$ PSF at low E_γ in spherical or weakly deformed nuclei, and is known as the KMF model. Despite the fact that there is no theoretical reason for this model to be applied in well deformed nuclei, it is often also adopted for these nuclei.

A second model was proposed for spherical nuclei by Chrien [13] in order to match the behavior of the SLO model at energies near the GEDR maximum and that of KMF model at very low E_γ. This phenomenological model was later generalized for deformed nuclei by Kopecky *et al.* [14] by introducing an empirical parameter k. The systematics of this parameter in [15] was based on the requirement to reproduce the total radiation widths of neutron resonances. As this quantity depends strongly on the model of the NLD below S_n as well as on the PSFs for other multipolarities, we considered the quantity k to be a free parameter in our simulations. This model is known as the EGLO (enhanced generalized Lorentzian) model and is very similar to the KMF model for $k \sim 1.5$.

In addition, many other models of the $E1$ PSF can be found in the literature. The RIPL-3 database [15] (probably the most widely used database by experimentalists) lists several additional closed-form models. These are the so-called hybrid model (GH) [16], the generalized Fermi liquid (GFL) model [17], and a family of modified Lorentzian (MLO) models; there are at least three different MLO models in the database. For a description of all of these models, the reader is referred to Ref. [15]. In addition, a PSF model based on Hartree-Fock-Bogoljubov (HFB) calculations can be found in RIPL-3. The authors of the RIPL-3 database recommend that the MLO models be used. All of the models mentioned (and several of their modifications) have been tested in our analysis. Many of these models use values of E_G, Γ_G, and σ_G as parameters. The same values of these parameters as in the SLO model were used in all of our analyses.

For a complete description of γ decay one needs information on the PSFs at all excitation energies. In some models, the dependence on any quantity other than E_γ is neglected, i.e., $f^{(\mathrm{XL})}(E_\gamma, \Theta)$ from Eq. (1) becomes $f^{(\mathrm{XL})}(E_\gamma)$. This assumption is known as the Brink hypothesis [18] and was formulated for $E1$ transitions originating from the giant electric dipole resonance (GEDR). Experimental data from average resonance capture seem to confirm at least the approximate validity of the hypothesis for γ-ray energies at about 6 MeV. Indications of the validity of the hypothesis have also been found for $M1$ scissors mode transitions [3,19,20].

From the above list of models, only the SLO model is assumed to follow the strict form of the Brink hypothesis. In addition, the hypothesis must also be used for the description of transitions between excited states in combination with the $E1$ PSF from HFB calculations. All other models predict a weak dependence of the PSF on the temperature T. This quantity is related to the excitation energy of the nucleus E via the relation $T = \sqrt{E/a}$; the parameter a is known as the level-density parameter.

The γ-ray energy dependence of the PSFs for several of these models of $f^{(E1)}$ is shown in Fig. 2. To keep the figure readable we do not show results for all of the models.

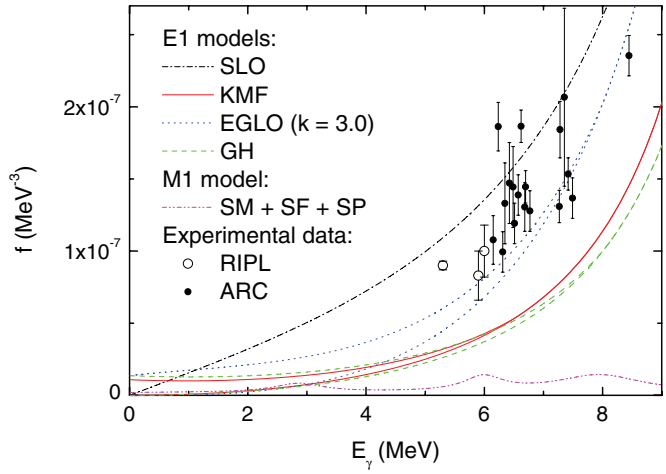

FIG. 2. (Color online) Photon strength functions as a function of γ-ray energy for some of the PSF models used in our simulations. The uncertainties are purely statistical. There are two curves for the KMF, EGLO, and GH models of the $E1$ PSF shown. They indicate how these models change as a function of temperature; the lower curve corresponds to $T = 0$ while the upper one to $T = \sqrt{(S_n - E_f)/a}$. For the $M1$ PSF the parameters of the scissors mode were $E_{\mathrm{SM}} = 2.9$ MeV, $\Gamma_{\mathrm{SM}} = 1.0$ MeV, and $\sigma_{\mathrm{SM}} = 0.2$ mb, and $f_{\mathrm{SP}}^{(M1)} = 2 \times 10^{-9}$ MeV^{-3}. Experimental data for $f^{(E1)}$ for ^{155,157,159}Gd at energies 5.9, 6.0, and 5.3 MeV, respectively, are from the RIPL database [34]. Data from average resonance capture in ^{155}Gd (ARC) are from Ref. [17].

2. *Magnetic dipole transitions*

Magnetic dipole ($M1$) transitions also play an important role in the decay of highly excited nuclear states below S_n. Usually, two models are used for $M1$ transitions. In the spin-flip (SF) resonance model, $f_{\mathrm{SF}}^{(M1)}(E_\gamma)$ is usually assumed to have a Lorentzian shape with an energy of about 7 MeV and a width of 4 MeV [15], while in the single-particle (SP) model, $f_{\mathrm{SP}}^{(M1)}$ is a constant independent of γ-ray energy. The $M1$ strength corresponding to the spin-flip mode was measured for several rare-earth nuclei (including ^{156}Gd) using inelastic proton scattering [21]. A double-humped structure was observed between 5 and 10 MeV and we adopted this form of the SF resonance in our simulations. The Lorentzian shape was used for these resonances.

Sometimes a sum of the strengths from the two models, $f_{\mathrm{SP}}^{(M1)}$ and $f_{\mathrm{SF}}^{(M1)}$, is used for the $M1$ PSF. In our simulations we usually adjusted the absolute value of the PSFs to obtain the ratio of $f^{(E1)}/f^{(M1)} \approx 7$ at 7 MeV. This value seems to be reasonably well determined from average resonance capture experiments [22]. If not specifically mentioned, the strict validity of the Brink hypothesis is assumed for these $M1$ models.

3. *Scissors mode*

In 1976, Hilton [23] and later Lo Iudice and Palumbo [24], using the geometrical two rigid rotors model, and Iachello [25],

using the proton-neutron interacting boson model, predicted an isovector $M1$ collective vibrational mode in deformed nuclei. This mode, known as the scissors mode (SM), was experimentally observed for ground-state transitions in ^{156}Gd by Bohle *et al.* [26] measured with high-resolution electron inelastic scattering at low momentum transfer. The parameters of the mode for transitions to the ground state were extensively investigated using the (γ,γ') reaction on rare-earth nuclei; this revealed substantial fragmentation of the mode. These experiments concluded that the strength of the mode (or more precisely the total $M1$ strength in the energy range $E_\gamma \approx 2.5$–4.0 MeV) for the ground-state transitions in even-even rare-earth nuclei is proportional to the square of the deformation [27]; for well deformed nuclei this strength reaches $B(M1) \approx 3\mu_N^2$. The published experimental values for ^{156}Gd are $B(M1) = 2.1(4)\mu_N^2$ [28], and $2.73(27)\mu_N^2$ [29]. In both cases, the strength corresponds to the energy range 2.7–3.7 MeV. The centroid of the scissors mode strength is located near 3 MeV and is almost constant in rare-earth nuclei; the experimental value for ^{156}Gd is $E_{\rm SM} = 3.060(7)$ MeV [30]. In our simulations the scissors mode was represented by a single Lorentzian resonance term.

Our recent analysis of multistep cascades from resonance neutron capture in ^{158}Gd [3] indicated that the width of the scissors mode in ^{158}Gd is in the range 0.6–1.6 MeV, and that the strength must be significantly smaller than the strength proposed from the (γ,γ') reaction. In addition, the SM must be combined not only with $f_{\rm SF}^{(M1)}$ but also with $f_{\rm SP}^{(M1)}$. The total $M1$ strength in the interval 2.5–4 MeV deduced from the analysis was at a maximum about $2\mu_N^2$. It was also observed that the parameters of the scissors mode determined from ^{3}He-induced reactions in even-even Dy isotopes [20] were not compatible with the parameters deduced from the ^{157}Gd(n,γ) reaction. It should be stressed that all of the results in ^{158}Gd were based on the assumption of the strict validity of the Brink hypothesis for the SM.

4. Electric quadrupole transitions

In addition to dipole transitions, electric quadrupole ($E2$) transitions might also play a role in the decay of neutron resonances. We found that $E2$ transitions are not important in the interpretation of our data; we adopted a simple single-particle model ($f_{\rm SP}^{(E2)} = $ constant) in our simulations. The strength of $f_{\rm SP}^{(E2)}$ was chosen to reproduce the ratio of partial radiation widths at about 7 MeV measured in average resonance capture experiments in deformed nuclei; this ratio is $\Gamma(E1)/\Gamma(E2) \gtrsim 100$ [22].

C. Nuclear Level density

There are many NLD models in the literature. We tested three different models for the energy dependence of the NLD. Two of them were given by closed-form formulas: (i) the back-shifted Fermi gas (BSFG), and (ii) the constant-temperature (CT) model [31]. There are two adjustable parameters in each of these models. Two different sets of these parameters were adopted for the BSFG as well as for the CT model. These sets correspond to two different parametrizations of both of these models, as found in the latest works of von Egidy and Bucurescu [31,32].

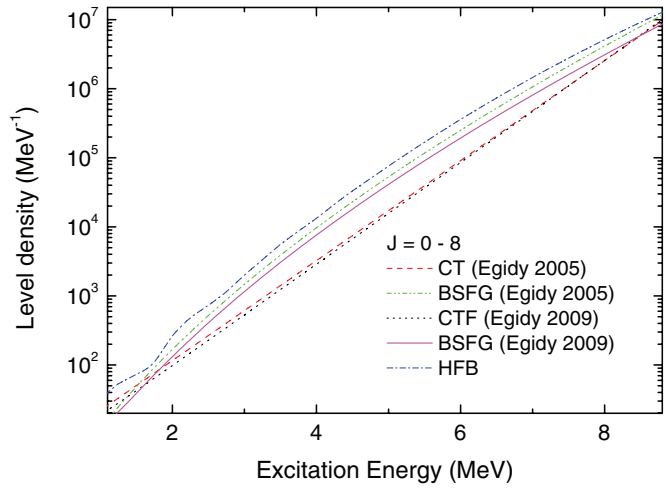

FIG. 3. (Color online) Level density models used in simulations for spin range $J = 0$–8. The different absolute values predicted by the various level density models originate from the different spin distributions for the different models. The resonance spacing of s-wave resonances is the same in all cases [15,31].

The spin dependence of the NLD for both of these models was the standard form [15,31]; no parity dependence was assumed above $E_{\rm crit}$.

In addition to these closed-form models, we tested the level density calculated within the Hartree-Fock-Bogoljubov (HFB) approach. In this approach the level density is available in tabulated form as a function of energy for levels with each spin and parity [15,33]. The calculated level densities usually suffer from difficulties in reproducing the average neutron resonance spacing. In order to bring the calculations into agreement with experimental data, the HFB level density was renormalized to reproduce the resonance spacing at the neutron separation energy [4]. After such a renormalization the HFB level density is similar to the BSFG model at energies above $E_{\rm crit}$; see Fig. 3.

All known levels below $E_{\rm crit} = 1.95$ MeV are taken into account in the simulations. The level density formula is thus applied only above this energy.

IV. RESULTS

A. MSC spectra

As already pointed out, to obtain information on the properties of the γ decay of ^{156}Gd we compared experimental MSC and gated MSC spectra with predictions based on model simulations described in Sec. III. The MSC spectra were constructed from capture on well resolved strong resonances. Only γ cascades that deposit virtually all of their energy in the DANCE detector, specifically 7.6–8.6 MeV, were taken into account and sorted according to cluster multiplicity. Multiplicities M = 2-7 were used in the analysis.

Experimental MSC spectra for several strong resonances are shown in Fig. 4. The errors shown are statistical errors. The spectra from resonances with the same spin are similar but not identical, due to Porter-Thomas fluctuations of the primary transitions. There is a strong peak at $E_\gamma \approx 1.1$ MeV in MSC spectra for all cluster multiplicities. This peak comes from decay of several levels (with both parities) with excitation

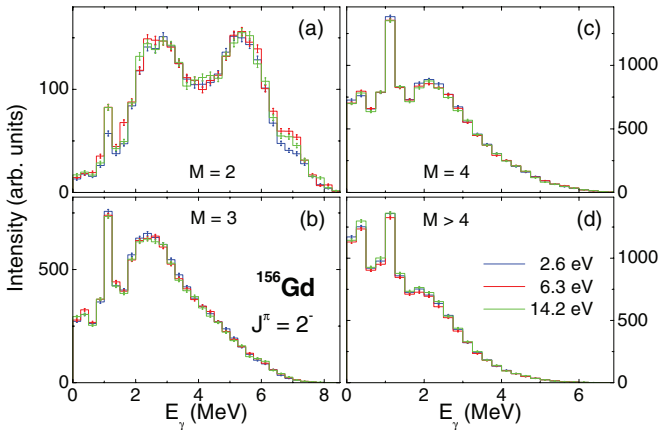

FIG. 4. (Color online) Experimental MSC spectra for three strong 2^- resonances.

energies of 1.1–1.5 MeV to the levels in the ground state rotational band. The levels just above 1 MeV are strongly populated during the γ decay of neutron resonances.

In order to clarify the role of the peak at 1.1 MeV, we constructed gated MSC spectra by selecting a gating γ-ray energy range 0.8–1.2 MeV; see Sec. II B. Examples of these spectra are shown in Fig. 5. As expected, selected gating produced a dip at about 1.0 MeV in these spectra.

To compare the gated MSC spectra with predictions based on various assumptions about PSFs, equivalent spectra were constructed accordingly from combined DICEBOX + GEANT4 simulations in a manner similar to that outlined above.

Gated MSC spectra are not independent of MSC spectra. The double-humped structure of these gated spectra for $M = 2$, see Fig. 5, is very interesting; see Sec. IV B3.

Several hundred model combinations of PSFs and NLD were tested in simulations and compared with the experimental spectra. It is very difficult to quantify the agreement between simulations and experimental spectra quantitatively as individual bins in the MSC and gated MSC spectra are mutually correlated in a complicated way, and the corresponding correlation is not known *a priori*. As a consequence, the degree of agreement was only checked visually.

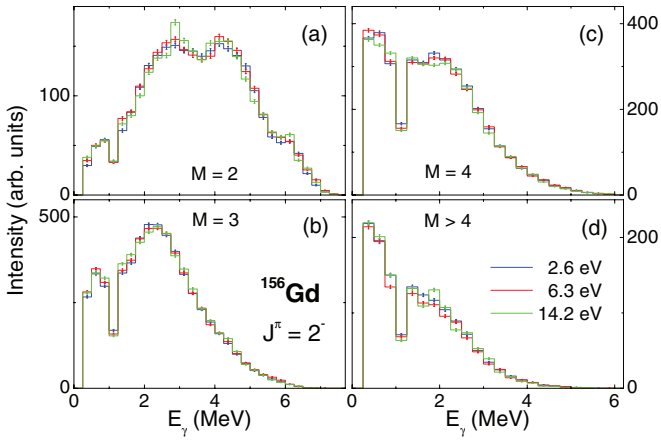

FIG. 5. (Color online) Experimental gated MSC spectra for several strong 2^- resonances.

The MSC and gated MSC spectra were binned into coarse bins with a width of 250 keV. Use of these relatively wide bins allows experimental uncertainties to be small and also suppresses the range of allowed predictions from different simulated nuclear realizations. The difference between nuclear realizations is mainly the consequence of the Porter-Thomas fluctuations of partial radiation widths.

To characterize uncertainties due to Porter-Thomas and level density fluctuations we plot an energy-dependent standard confidence region of the spectral intensity, characterizing the behavior of this set. This confidence region is plotted in Figs. 6–8 as a gray band. Each band has a width of two sigma (the average $\pm$ one sigma) with the mean and sigma taken from the 20 realizations. The size of fluctuations among the spectra for different resonances is reasonably well reproduced by the simulations. The spectra from different nuclear realizations are almost identical for higher multiplicities ($M \geqslant 4$), while some differences are predicted for lower multiplicities, especially for $M = 2$.

B. Comparison with experiment

Within an enormous functional space the trial-and-error method adopted in our analysis does not guarantee that we find the models or combinations of model parameters that lead to the best agreement between simulated and experimental (gated) MSC spectra. In practice we have found only a few combinations of PSF and NLD models which lead to acceptable reproduction of the experimental spectra. Although comparison for only one resonance spin ($J^{\pi} = 1^-$) is shown in Figs. 6–8, the results are independent of resonance spin.

1. Electric dipole PSF

Reasonably good agreement could be found with the KMF and GH models, as well as with the EGLO model (with the phenomenological parameter k adjusted at values $\sim$1.5–3.0), in a particular combination with $M1$ and level density models; see below. The fact that KMF and GH models yielded similar results is not surprising as the shapes of PSFs for these two models are similar; see Fig. 2.

On the other hand, if SLO, MLO (with the exception of MLO1), or $f^{(E1)}$ from HFB calculations were used, there was a striking disagreement between experimental and simulated spectra in all cases. Also the best agreement between simulations and experiment obtained with GFL and MLO1 models is significantly worse than in the case of KMF, GH, and EGLO models (although much better than with SLO and HFB models).

There are two important common features of all acceptable $E1$ models. First, the PSF (at least for transitions between excited states) is relatively flat at γ energies at which we are sensitive. There are only a limited number of primary transitions to levels at very low excitation energies, which makes the analysis almost insensitive to $E_\gamma \gtrsim$ 6–7 MeV. Any $f^{(E1)}$ model that shows an increase with E_γ similar to the SLO model at $E_\gamma \lesssim$ 6–7 MeV generates more transitions with higher energies. This leads to a multiplicity distribution shifted to smaller values than observed experimentally.

Second, all acceptable models are temperature dependent. Consequently, they violate the strict form of the Brink

hypothesis. In order to check whether we absolutely need a temperature-dependent $E1$ PSF in order to reproduce the MSC spectra we also performed simulations with a "modified" KMF model. In these simulations we did not let the temperature T of the state be a function of excitation energy, but instead fixed T and used it as an additional model parameter. We found that for a very limited range of the temperature T, specifically for T between about 0.30 and 0.35 MeV, the simulations reproduced experimental spectra similar to those for the standard KMF model. These results indicate that the question whether the PSF depends on excitation energy for energies at the low-energy tail of GEDR cannot be unambiguously answered from the present study of resonance neutron capture.

2. *Nuclear level density*

As already mentioned in Sec. III C, two different parametrizations of BSFG and CT models were tested. The results with the two different parametrizations of the corresponding NLD model are very similar. In addition, results with the HFB model are also very similar to the closed-form BSFG models. This could be expected from the similar energy dependences of these models; see Fig. 3.

We were unable to reproduce the experimental spectra using the CT model of the NLD with any of the PSF models that we tried. Simulations with the CT model give a clear shift in the multiplicity distribution toward lower values as compared to those obtained with the BSFG model. This feature might be expected from the NLD energy dependence shown in Fig. 3: the ratio of available levels at very low excitation energy with respect to higher energies (near 4 MeV) is higher for the CT model, which causes a suppression of transitions with lower energies with respect to BSFG. This leads to a stronger preference for low multiplicities in the CT model, in disagreement with the experimental results.

3. *Magnetic dipole PSF*

The experimental MSC and gated MSC spectra for multiplicity $M = 2$ in Figs. 4 and 5 clearly show a double-humped shape with maxima close to $E_\gamma = 3$ and 5 MeV. These maxima, as well as the shapes of $M = 3$ spectra near $E_\gamma = 3$ MeV cannot be reproduced with a model without a resonance structure near this energy. A typical example of simulated MSC spectra with no such resonance structure is shown in Fig. 6.

The shape of the experimental gated MSC spectra for $M = 2$ implies that the resonance structure in a PSF must also inevitably play a role in transitions ending at levels with excitation energy between 1.1 and 1.5 MeV. Gated MSC spectra thus demonstrate that the resonance structure must also be postulated for transitions between excited states, i.e., they strongly indicate that the Brink hypothesis is valid for the resonance structure near 3 MeV.

Comparison of simulations with experimental MSC spectra for $M = 2$ clearly shows that this resonance structure cannot be purely of $E1$ character. The difference in predicted spectra for a resonance structure in $E1$ and $M1$ arises from the fact that the $M = 2$ spectrum consists mainly of events where neutron resonances with negative parity decay via two γ rays to the ground state with positive parity. If $E1$ strength dominated the

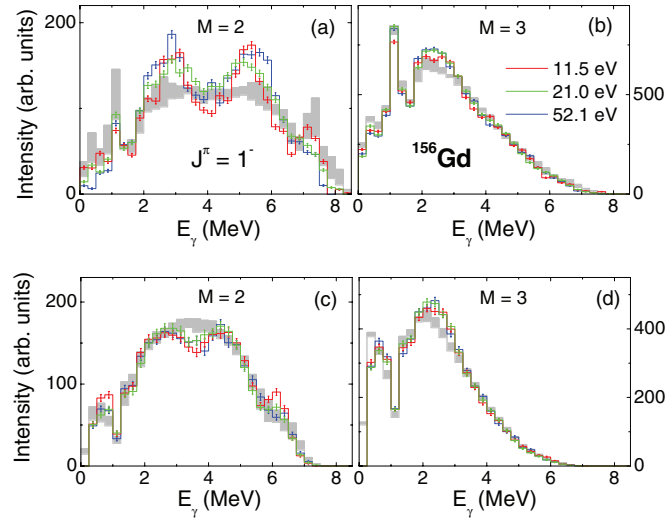

FIG. 6. (Color online) Comparison of experimental MSC spectra [(a) and (b)] and gated MSC spectra [(c) and (d)] with simulations in which the scissors mode was completely absent for resonances with $J^\pi = 1^-$. Predictions of simulations are represented as a gray band. The KMF model was used for the $E1$ PSF while the BSFG model was used for the level density.

PSF near 3 MeV (which would be the case if the resonance-like structure was in the $E1$ PSF), such decays with $M = 2$ would not be possible.

On the other hand, distinguishing between $M1$ and $E2$ character of the structure is more complicated due to the same parity selection rules for these types of transitions. Nevertheless, simulations with a resonance structure postulated in the $E2$ PSF yielded slightly worse agreement. If this finding is combined with expectation of the presence of the $M1$ SM and no prediction of strong transitions with $E_\gamma \approx 3$ MeV of $E2$ character, we believe that the structure in PSF near $E_\gamma = 3$ MeV corresponds to this $M1$ SM.

Assuming that the SM consists of a single-Lorentzian term, we found that the MSC spectra are rather sensitive to the energy of the centroid of the SM $E_{\rm SM}$. It must be very close to 3 MeV; we found that it cannot be lower than about 2.7 MeV or higher than about 3.1 MeV. If the energy of the mode is outside of this range the shapes of the bumps in the MSC spectra for $M = 2$–3 are not reproduced.

The best simultaneous description of MSC and gated MSC spectra seems to be reached with an energy of the mode $E_{\rm SM} \sim 2.9$ MeV. MSC spectra, especially those for $M = 2$, are best described with $E_{\rm SM} \sim 3.0$ MeV while gated MSC spectra indicate $E_{\rm SM} \sim 2.8$ MeV. There is a question whether this small difference in $E_{\rm SM}$ may indicate a shift of the position of the mode with excitation energy. We tried to test this possibility by introducing a linear dependence of the position of the scissors mode on excitation energy. However, with this model we never reached the quality of predictions that assume fixed energy. Only simulations with BSFG and HFB models yielded acceptable agreement with experimental spectra.

As for the damping width of the scissors mode, $\Gamma_{\rm SM}$, the data seem to allow $\Gamma_{\rm SM} \approx 0.8$–1.4 MeV. There are additional constraints. For instance, the shape of the gated MSC spectrum

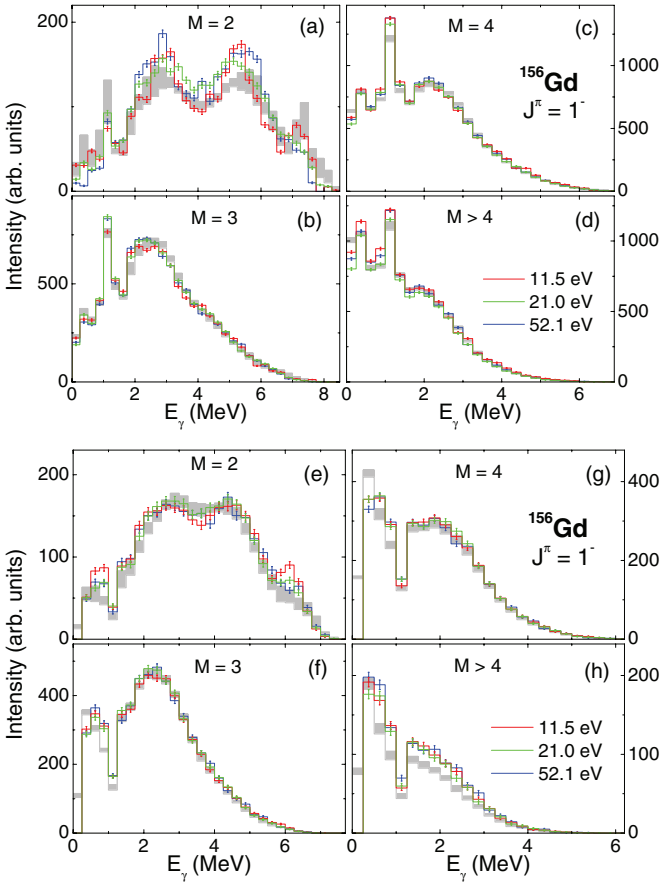

FIG. 7. (Color online) Comparison of experimental MSC spectra [(a)–(d)] and gated MSC spectra [(e)–(h)] with simulations for $J^\pi = 1^-$ resonances (gray band). The model combination of $f^{(E1)}_{\rm KMF}$, $f^{(M1)}_{\rm SM} + f^{(M1)}_{\rm SP} + f^{(M1)}_{\rm SF}$ is used. The parameters of the scissors mode were $E_{\rm SM} = 2.9$ MeV, $\Gamma_{\rm SM} = 1.0$ MeV, $\sigma_{\rm SM} = 0.2$ mb, and $f^{(M1)}_{\rm SP} = 2 \times 10^{-9}$ MeV^{-3}. As noted in the text, only simulations with BSFG and HFB models yielded acceptable agreement with experimental spectra.

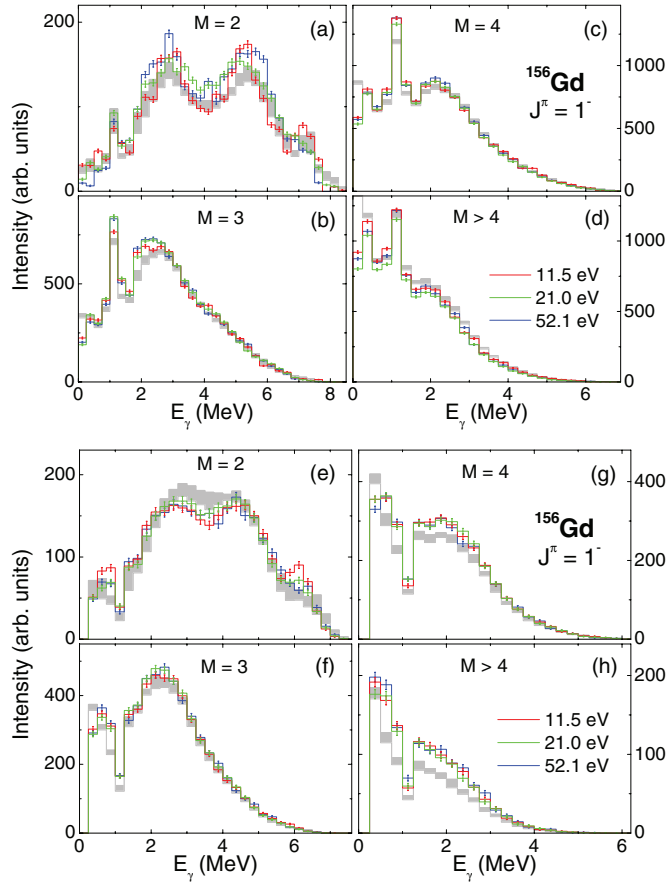

FIG. 8. (Color online) The same as in Fig. 7 but for the EGLO model of $E1$ PSF (with $k = 3.0$).

for $M = 2$ indicates that, if the position of the scissors mode is between 2.9 and 3.0 MeV, the damping width of the resonance cannot be higher than about 1.0 MeV.

Models for which $f^{(M1)}$ consisted only of SM or SM + SF did not lead to reasonable agreement between simulations and experiment. The problem with the reproduction of spectra with these models arises with the relative size of bumps near 3 MeV in multiplicity $M = 2$ and $M = 3$ spectra: if the strength of the SM was adjusted to reproduce bumps in $M = 2$ spectra, the bump in $M \geqslant 3$ near 3 MeV was in all cases too large. On the other hand, if the spectra in $M \geqslant 3$ are reasonably well reproduced, then bumps in the $M = 2$ spectra are too small. The only simulations that reasonably reproduced the bumps for all multiplicities were those using a "composite" model of the $M1$ PSF: $f^{(M1)} = f^{(M1)}_{\rm SM} + f^{(M1)}_{\rm SF} + f^{(M1)}_{\rm SP}$.

Even with this model the description of the experimental data is not perfect. As seen from Figs. 7 and 8, only about 70% of the intensity in the bumps in $M = 2$ spectra can be explained with this model. In principle, we are able to reproduce bumps in $M = 2$ spectra, but this leads to insurmountable problems in spectra for all other multiplicities. We are unable to explain the missing predicted strength in the bumps in the $M = 2$ spectra.

In any case we emphasize that reasonable simultaneous descriptions of MSC and gated MSC spectra for all multiplicities, i.e., of many different observables, seems to justify our view of the compound nucleus and the photon strength functions in deformed rare-earth nuclei. Note that the fluctuations among the experimental spectra from different resonances are consistent with the fluctuations predicted from DICEBOX+GEANT4 simulations, as Figs. 6–8 demonstrate. This observation also indicates that the fluctuation properties assumed in the statistical description of the nucleus (e.g., Porter-Thomas fluctuations) are correct.

As simulated spectra are sensitive only to relative values of PSFs for different types of transitions, one might expect that the absolute values of $f^{(M1)}$ will depend on the adopted model of $E1$ PSF. All allowed $E1$ models, see Sec. IV B1, have rather similar energy dependences as well as absolute values (see Sec. IV B1). As a consequence the allowed parameters of $f^{(M1)}$ are almost independent of the $E1$ model. The higher the absolute value of the $E1$ PSF near 3 MeV, the higher the needed value of the $M1$ PSF. The allowed value of $f^{(M1)}_{\rm SP}$ can be within the range $\approx$2–4 $\times 10^{-9}$ MeV^{-3}, and the maximum cross section of the scissors mode $\sigma_{\rm SC} \approx 0.07$–$0.32$ mb (more precisely, $\sigma_{\rm SC} \approx 0.07$–$0.25$ mb and $\approx$0.15–0.32 mb for the KMF and EGLO models, respectively). The values of all other

parameters have already been specified. Examples of predicted MSC spectra for two model combinations, which reproduce the experimental spectra reasonably well, are shown in Figs. 7 and 8, with the set of parameters for the $f^{(M1)}$ PSF specified in the figure caption.

We cannot guarantee that the scissors mode can be described with a single-Lorentzian resonance. But descriptions of the mode with more complex resonance structures do not significantly improve the agreement between simulations and experiment. We also cannot guarantee that the properties of the scissors mode completely follow the Brink hypothesis. For example, the properties of the mode for ground-state transitions might differ from the properties of the mode build on all other levels. Simulations yield the same degree of agreement if the strength of the SM for ground state transitions is increased by an arbitrary factor or left unchanged.

V. COMPARISON WITH OTHER DATA

There are several relevant measurements that provide information on the PSFs at the low-energy tail of the GEDR either directly in ^{156}Gd or for other well deformed nuclei in the $A \sim 155$–160 mass region.

First, there are extensive data from the (n,γ) reaction. Specifically, (i) values of the PSFs were obtained from the intensities of primary transitions from resonance neutron capture in neighboring odd nuclei [34], (ii) information on the PSFs was obtained for ^{158}Gd from analysis of MSC spectra [3], (iii) data from a neutron average-resonance capture experiment on ^{155}Gd have been published [17], and (iv) information on the total radiation widths of neutron resonances is available for all stable isotopes [35]. In addition, we have preliminary results from analysis of odd Gd isotopes measured with the DANCE detector [36].

Apart from the (n,γ) reaction, data on ground-state transitions from (γ,γ') [28,29], and (e,e') [26] measurements are available for ^{156}Gd, while data from ^{3}He-induced reactions [20] are available for three even-even Dy isotopes.

The model parameters obtained from analysis of the MSC and gated MSC spectra in ^{156}Gd are almost identical to those reproducing MSC spectra in ^{158}Gd [3]. This finding indicates that the PSFs and NLD parameters are very similar for nuclei with a similar mass and deformation. As a consequence, some problems arising from comparison with data from other reactions remain unexplained. It means, e.g., that the position of the scissors mode reported from analysis of the $(^{3}\mathrm{He},\alpha)$ reaction on even-even Dy nuclei is too low compared to the value allowed by our data; see [3].

In our previous analysis of ^{158}Gd [3] we did not test models with $f^{(M1)} = f^{(M1)}_{\mathrm{SM}} + f^{(M1)}_{\mathrm{SF}} + f^{(M1)}_{\mathrm{SP}}$ where $f^{(M1)}_{\mathrm{SP}} \gtrsim 2.5 \times 10^{-9}$ MeV^{-3}. Additional simulations for ^{158}Gd with these model parameters indicate that the set of parameters describing the MSC spectra for ^{156}Gd is also able to describe the MSC spectra for ^{158}Gd.

The sum of reduced transition probabilities of magnetic-dipole transitions from the ground state to the energy region 2.7–3.7 MeV that was observed in the (γ,γ') measurement is comparable to the value obtained from simulations with a maximum allowed $f^{(M1)}$ strength. Specifically, a model with $f^{(M1)}_{\mathrm{SP}} = 4 \times 10^{-9}$ MeV^{-3}, $\Gamma_{\mathrm{SC}} = 1.0$ MeV, and $\sigma_{\mathrm{SC}} = 0.3$ mb corresponds to about $2.8\mu_N^2$ in this energy interval. This value agrees with the value $2.73(27)\mu_N^2$ [29]. However, it should be noted that in our simulations only about half of the simulated value comes from the SM, and that the values of reduced transition probabilities from the (γ,γ') reaction in other deformed even-even nuclei are usually higher than $3\mu_N^2$ [29]. As mentioned at the end of the previous section, we cannot distinguish from our simulations whether the strength of the ground state SM is exactly the same as for the SM built on the excited states or if it differs by an arbitrary factor.

None of the acceptable $E1$ models (KMF, GH, EGLO) is able to completely reproduce the $E1$ PSF inferred from the intensities of primary transitions from (n,γ) reactions on ^{155}Gd and neighboring odd nuclei; see Fig. 2. Since there is no odd-even A effect observed experimentally in the $f^{(E1)}$ PSF above the neutron separation energy, it seems reasonable to expect similar values of $f^{(E1)}$ in odd and even-even nuclei at about 6 MeV. Of these three models, the best agreement with data from [17,34] is reached with the EGLO model with the value of the parameter k close to 3.0.

The total radiation widths of neutron resonances, Γ_γ, predicted with the best KMF, GH, and EGLO (with $k \approx 3.0$) models for $E1$ are 80–90, 80–90, and 115–130 meV, respectively. The predicted value of Γ_γ depends on the detailed parameters of $f^{(M1)}$ and NLD. Values simulated for the EGLO model are in excellent agreement with available experimental data: $\Gamma_\gamma^{(\mathrm{exp})} = 120(3)$ [4] or 110(3) meV [35]. This finding again prefers the EGLO model of the $E1$ PSF over other models. The predicted fluctuation of Γ_γ among different resonances is small, both among resonances with the same spin as well as between resonances with spins 1^- and 2^-; at most about 5 meV.

It should be emphasized that the total radiation width is the only one of the simulated quantities that depends on the absolute value of the PSFs. All other observables depend only on ratios of the PSFs for different types of transitions and on their energy dependence, but not on the absolute values. A reasonable reproduction of Γ_γ could thus be obtained not only with the EGLO ($k \sim 3$) model, but also if model combinations with the KMF or GH models are multiplied by a factor of 1.4. This would correspondingly increase the $M1$ strength; the total $B(M1)$ strength in the region 2.7–3.7 MeV would then be close to $3\mu_N^2$. This is comparable to values obtained from the (γ,γ') experiments, but still slightly smaller than values for the majority of well deformed nuclei.

In any case the present status of knowledge of the PSFs is far from desirable; it seems very difficult to reproduce all available experimental data on PSFs in the rare-earth region. Our analysis indicates that out of the tested models the best description of the $E1$ PSF can be reached with the EGLO model (with $k \approx 3$).

VI. SUMMARY

A measurement of γ-ray spectra from resonances in the ^{155}Gd(n,γ) reaction was performed with an isotopically enriched target at the DANCE detector array at the LANSCE spallation neutron source.

The MSC and gated MSC γ-ray spectra for different multiplicities from resonances with different spins were used to test the validity of various PSFs and NLD models for ^{156}Gd. Results for this nucleus are consistent with results obtained from analysis of MSC spectra of another deformed even-even Gd isotope, ^{158}Gd [3]. In addition, a reasonable simultaneous description of all experimental spectra together with satisfactory descriptions of the fluctuation properties, indicate that the standard picture of the compound nucleus and the PSFs are valid for deformed rare-earth nuclei.

Our data indicate that, for the $E1$ PSF at energies below about 6 MeV, a reasonable description can be obtained with the model of Kadmenskij, Markushev, and Furman [12] or with models having a similar γ-ray energy dependence. Models of the $E1$ PSF with a steeper γ-ray energy dependence (similar to a Lorentzian shape) at these energies are not acceptable. If all available experimental data are taken into account, the best description of the $E1$ PSF is with models similar to the EGLO model. The temperature dependence of the $E1$ PSF predicted by these models does not appear to be required.

The presence of the $M1$ resonance near 3 MeV, which is identified with the scissors mode, is necessary for describing the behavior of the γ cascades ending at the ground state, as well as at excited levels. Although the strength of the scissors mode alone is significantly smaller than the strength observed in the NRF experiments, the total $M1$ strength at $E_\gamma \approx 3$ MeV needed for description of our data is similar to that observed in the NRF experiments.

The energy dependence of the nuclear level density is reasonably well described with the BSFG model, while the dependence predicted by the CT model is highly improbable.

In conclusion, not all problems with the PSFs and level density in deformed nuclei are resolved; further study of these quantities is clearly needed.

ACKNOWLEDGMENTS

This work was supported in part by the US Department of Energy Grants No. DE-NA0001784 and No. DE-FG02-97-ER41042. This work benefited from the use of the LANSCE accelerator and was performed under the auspices of the US Department of Energy at Los Alamos National Laboratory by Los Alamos National Security, LLC, under Contract No. DE-AC52-06NA25396. It was also supported by the research plans MSM 0021620859 and LG13013 of the Ministry of Education of the Czech Republic, and Grant No. 13-07117S of the Czech Science Foundation.

[1] M. Heil, R. Reifarth, M. M. Fowler, R. C. Haight, F. Käppeler, R. S. Rundberg, E. H. Seabury, J. L. Ullmann, and K. Wisshak, Nucl. Instrum. Methods Phys. Res., Sect. A **459**, 229 (2001).
[2] R. Reifarth *et al.*, Nucl. Instrum. Methods Phys. Res., Sect. A **531**, 530 (2004).
[3] A. Chyzh *et al.*, Phys. Rev. C **84**, 014306 (2011).
[4] B. Baramsai *et al.*, Phys. Rev. C **85**, 024622 (2012).
[5] P. W. Lisowski *et al.*, Nucl. Sci. Eng. **106**, 208 (1990).
[6] J. M. Wouters *et al.*, IEEE Trans. Nucl. Sci. **53**, 880 (2006).
[7] F. Bečvář, Nucl. Instrum. Methods Phys. Res., Sect. A **417**, 434 (1998).
[8] M. Jandel *et al.*, Nucl. Instrum. Methods Phys. Res., Sect. B **261**, 1117 (2007).
[9] C. W. Reich, Nucl. Data Sheets **99**, 753 (2003).
[10] C. E. Porter and R. G. Thomas, Phys. Rev. **104**, 483 (1956).
[11] S. S. Dietrich and B. L. Berman, At. Data Nucl. Data Tables **38**, 199 (1988).
[12] S. G. Kadmenskij, V. P. Markushev, and V. I. Furman, Sov. J. Nucl. Phys. **37**, 165 (1983).
[13] R. E. Chrien, in *Proceedings of the Vth International School on Neutron Physics, Alushta, Dubna 1987*, edited by B. B. Kolesova and V. R. Sarantseva, Dubna Report No. D3, 4, 17-86-747 (JINR, Dubna, Russia, 1987).
[14] J. Kopecky, M. Uhl, and R. E. Chrien, Phys. Rev. C **47**, 312 (1993).
[15] R. Capote *et al.*, Nucl. Data Sheets **110**, 3107 (2009).
[16] S. Goriely, Phys. Lett. B **436**, 10 (1998).
[17] S. F. Mughabghab and C. L. Dunford, Phys. Lett. B **487**, 155 (2000).
[18] D. M. Brink, Ph.D. thesis, Oxford University, 1955 (unpublished).
[19] M. Krtička, F. Bečvář, J. Honzátko, I. Tomandl, M. Heil, F. Käppeler, R. Reifarth, F. Voss, and K. Wisshak, Phys. Rev. Lett. **92**, 172501 (2004).
[20] A. Schiller, A. Voinov, E. Algin, J. A. Becker, L. A. Bernstein, P. E. Garrett, M. Guttormsen, R. O. Nelson, J. Rekstad, and S. Siem, Phys. Lett. B **633**, 225 (2006).
[21] D. Frekers *et al.*, Phys. Lett. B **244**, 178 (1990).
[22] L. M. Bollinger and G. E. Thomas, Phys. Rev. C **2**, 1951 (1970).
[23] R. R. Hilton, in *Proceedings of the International Conference on Nuclear Structure, Dubna, 1976* (unpublished).
[24] N. Lo Iudice and F. Palumbo, Phys. Rev. Lett. **41**, 1532 (1978).
[25] F. Iachello, Nucl. Phys. A **358**, 89c (1981).
[26] D. Bohle *et al.*, Phys. Lett. B **137**, 27 (1984).
[27] W. Ziegler, C. Rangacharyulu, A. Richter, and C. Spieler, Phys. Rev. Lett. **65**, 2515 (1990).
[28] H. H. Pitz, U. E. P. Berg, R. D. Heil, U. Kneissl, R. Stock, C. Wesselborg, and P. von Brentano, Nucl. Phys. A **492**, 411 (1989).
[29] U. Kneissl, H. H. Pitz, and A. Zilges, Prog. Part. Nucl. Phys. **37**, 349 (1996).
[30] N. Pietralla *et al.*, Phys. Rev. C **58**, 184 (1998).
[31] T. von Egidy and D. Bucurescu, Phys. Rev. C **72**, 044311 (2005).
[32] T. von Egidy and D. Bucurescu, Phys. Rev. C **80**, 054310 (2009).
[33] S. Goriely, Nucl. Phys. A **605**, 28 (1996).
[34] J. Kopecky, in *Handbook for Calculations of Nuclear Reaction Data*, Report No. IAEA-TECDOC-1034 (IAEA, Vienna, 1998), p. 97.
[35] S. F. Mughabghab, *Atlas of Neutron Resonances* (Elsevier, Amsterdam, 2006).
[36] J. Kroll *et al.*, Eur. Phys. J. Web Conf. **21**, 04005 (2012).